



HAL
open science

Interfacial liquid water on Mars and its potential role in formation of hill and dune gullies.

Konrad J. Kossacki, Wojciech J. Markiewicz

► To cite this version:

Konrad J. Kossacki, Wojciech J. Markiewicz. Interfacial liquid water on Mars and its potential role in formation of hill and dune gullies.. *Icarus*, 2010, 210 (1), pp.83. 10.1016/j.icarus.2010.06.029 . hal-00683834

HAL Id: hal-00683834

<https://hal.science/hal-00683834>

Submitted on 30 Mar 2012

HAL is a multi-disciplinary open access archive for the deposit and dissemination of scientific research documents, whether they are published or not. The documents may come from teaching and research institutions in France or abroad, or from public or private research centers.

L'archive ouverte pluridisciplinaire **HAL**, est destinée au dépôt et à la diffusion de documents scientifiques de niveau recherche, publiés ou non, émanant des établissements d'enseignement et de recherche français ou étrangers, des laboratoires publics ou privés.

Accepted Manuscript

Interfacial liquid water on Mars and its potential role in formation of hill and dune gullies.

Konrad J. Kossacki, Wojciech J. Markiewicz

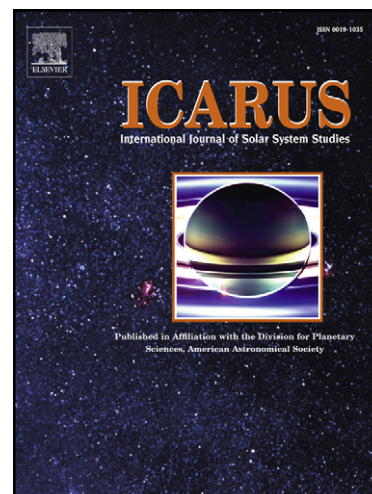
PII: S0019-1035(10)00251-4
DOI: [10.1016/j.icarus.2010.06.029](https://doi.org/10.1016/j.icarus.2010.06.029)
Reference: YICAR 9481

To appear in: *Icarus*

Received Date: 10 February 2010
Revised Date: 22 June 2010
Accepted Date: 23 June 2010

Please cite this article as: Kossacki, K.J., Markiewicz, W.J., Interfacial liquid water on Mars and its potential role in formation of hill and dune gullies., *Icarus* (2010), doi: [10.1016/j.icarus.2010.06.029](https://doi.org/10.1016/j.icarus.2010.06.029)

This is a PDF file of an unedited manuscript that has been accepted for publication. As a service to our customers we are providing this early version of the manuscript. The manuscript will undergo copyediting, typesetting, and review of the resulting proof before it is published in its final form. Please note that during the production process errors may be discovered which could affect the content, and all legal disclaimers that apply to the journal pertain.



Interfacial liquid water on Mars and its potential role in formation of hill and dune gullies.

Konrad J. Kossacki^a Wojciech J. Markiewicz^b

^a*Institute of Geophysics of Warsaw University,
Pasteura 7, 02-093 Warsaw, Poland*

^b*Max Planck Institute for Solar System Research,
Max-Planck-Str 2, D-37191 Katlenburg-Lindau, Germany*

Abstract

Gullies are among the most intriguing structures identified on the surface of Mars. Most common are gullies located on the slopes of craters which are probably formed by liquid water transported by shallow aquifers (Heldmann et al., 2007). Two particular types of gullies are found on slope of isolated hills and dunes. The hill-slope gullies are located mostly at 50° S, which is at the high end of latitudes of bulk of the gullies found so far. The dune gullies are found in several locations up to 65°S (Reiss et al., 2007), but the best known are those in Russel crater at 54° S. The hill-and dune gullies are longer than others making the aquifers explanation for their formation unlikely (Balme et al., 2006). Recently it has been noted that thin liquid films of interfacial water can play a role in rheological processes on the surface of Mars (Moehlmann, 2008; Kereszturi et al., 2009). Here we try to answer the question whether interfacial liquid water may occur on Mars in quantities large enough to play a role in formation of gullies. To verify this hypothesis we have calculated thermal models for hills and dunes of various steepness, orientation and physical properties. We find that within a range of average expected values of parameters it is not possible to have more than a few monolayers of liquid water at depths greater than a centimeter. To create subsurface interfacial water film significantly thicker and hence to produce conditions for the slope instability, parameters have to be chosen to have their extreme realistic values or an additional source of surface heating is needed. One possibility for additional heating is a change of atmospheric conditions due to a local dust storm. We conclude that if interfacial water is responsible for the formation of the hill-slope gullies, our results may explain why the hill gullies are rare.

Key words: Mars, Surface, Water

1 Introduction

2 Water has always been one of the central themes in studies of Mars. Stability of
3 liquid water has been investigated by many authors. Some researches suggest,
4 that water can be stable almost everywhere (Hecht, 2002), while others argue it
5 is unstable everywhere (Mellon and Philips, 2001). There is however one form
6 of liquid water which is undoubtedly stable under practically all conditions.
7 This so called unfrozen or interfacial water is a thin liquid film separating
8 frozen water ice and any mineral surface wherever these are present. The key
9 question is how thick this layer can be. In recent studies it has been proposed
10 that interfacial liquid water can be responsible for surface rheological processes
11 on Mars (Moehlmann, 2008; Kereszturi et al., 2009). Here we attempt to model
12 both the diurnal and the seasonal cycle of the interfacial liquid water in the
13 context of a possible mechanism for formation of the so called hill gullies. If
14 the subsurface liquid interfacial is thick enough it could destabilize the surface
15 layers and produce the observed gullies.

16 Gullies are among the most intriguing structures identified on the surface
17 of Mars (Malin and Edgett, 2000). Since the time of their discovery, gullies
18 were investigated by many authors (e.g. Mellon and Philips (2001); Costard et
19 al. (2002); Christensen (2003); Kossacki and Markiewicz (2004); Balme et al.
20 (2006); Heldmann et al. (2007); Reiss et al. (2010)). To date these structures
21 have been found in hundreds of locations in both hemispheres, incised into
22 slopes in different types of terrain, impact craters, pits and valleys, hills and
23 even dunes. In the current work we look only at the hill- and dune-gullies. In a
24 survey of the southern hemisphere by Balme et al., (2006) the hill gullies were
25 identified at latitudes about 30°S - 60°S , almost exclusively at the bottom of
26 the Argyre basin and Gorgonum Chaos. These authors found that about 10%
27 of gullied slopes visible in MOC images and about 23% in HRSC images are
28 hill slopes. This in turn translates to nearly 100 hills identified to have gullies
29 on their slopes. In Fig. 1 we show an example of a gullied hill, located in the
30 South, approximately at 47.25°S , 330.1°E . This hill is about 2 km across, and
31 about 1 km high. The dune gullies were found on numerous dark dunes in the
32 southern hemisphere, up to 65°S (Reiss et al., 2007). According to Fenton
33 (2006) flow features are observed on dune slopes inclined by about 30° , are up
34 to hundreds of meters long and a few meters wide. Best known are probably
35 the dune gullies in Russel crater at 54.5°S , studied by numerous authors (e.g.
36 Mangold et al. (2003); Reiss et al. (2010)). These gullies have lengths of about
37 2 km and a relatively constant width of about 10 m. The channels are of
38 sinuous shape and have branches, mostly in the upper sections. The listed set
39 of features match scenario of the formation by viscous slurry flows (Mangold
40 et al., 2003). Calculated velocities and viscosities are in the range of terrestrial

Email address: E-mail: kjkossac@fuw.edu.pl (Konrad J. Kossacki).

41 debris flows (Miyamoto et al., 2004). The channels are formed on the dune
42 slope of the gradient only about 10° , too low for a debris flow (Mangold et al.,
43 2003).

44 The physical processes involved in the formation of gullies are still under
45 debate. In the literature various possibilities are discussed, mostly involving
46 liquid water. Gullies located on the slopes of impact craters, by far the largest
47 population, are most likely formed by liquid water, probably transported by
48 shallow aquifers (Heldmann et al., 2007). The gullies found on the slopes of
49 isolated hills, or dunes seem to be of different origin. The hill gullies are on
50 average 50% longer than crater dunes, contradicting curving of gullies by water
51 flowing from underground aquifer hypothesis, because only a small amount
52 of water may be stored within an isolated hill (Balme et al., 2006). The same
53 conclusion can be drawn for dune gullies. Here, we investigate the possibility
54 that the slopes of gullied hills and dunes can become unstable due to interfacial
55 melting of subsurface water ice, as suggested by observations of growing flow-
56 like features on dunes (Moehlmann and Kereszturi, 2010; Kereszturi et al.,
57 2010). Thickness of the water liquid film between a mineral grain and the
58 ice layer is determined by the van der Waals force and is strongly dependent
59 on the temperature. Theoretically one or two monolayers of this unfrozen
60 water are present under any Martian conditions (Moehlmann, 2008). However,
61 significant thickness of the water film can be expected only at temperatures
62 close to the melting temperature of the ice. Thus, interfacial melting should be
63 most important in locations where: a) the temperature does not reach melting
64 point, but can be close to it; or b) ice is present mostly at night time, sublimates
65 away before it can melt and later condenses again from the vapor phase.

66 The highest temperatures are encountered on surfaces illuminated at low
67 zenith angle, but in such locations ice can be present only at some depth.
68 To determine thickness of the interfacial water film realistic for the Martian
69 regolith it is necessary to calculate distribution of the temperature and the
70 water ice simultaneously. We have used such models in other contexts in the
71 past (e.g. Kossacki and Markiewicz (2004)). Here we build on these models by
72 including the equation for the interfacial liquid water. In the next section we
73 briefly describe the model used and relevant range of the physical parameters.
74 This is followed by results for hill slopes of different orientations and inclina-
75 tions as well as a range of thermal and optical properties of the regolith. We
76 conclude with discussion of the results.

77 **2 Model description**78 *2.1 Basic features*

79 We used a numerical model that simulates evolution of the regolith temper-
80 ature, as well as condensation and sublimation of H₂O and CO₂ ices. The
81 model was previously used to investigate the possibility of seasonal ice melt-
82 ing in Martian gullies (Kossacki and Markiewicz, 2004), to simulate the escape
83 rate of subsurface ice (Kossacki et al., 2006), and to investigate possible frost
84 formation in small trenches dug during the Phoenix mission (Kossacki and
85 Markiewicz, 2009). In the current version we added formation of water film
86 between the regolith grains and the water ice mantling the grains, see Sec-
87 tion 2.2.

88 Our model describes diurnal and seasonal condensation and sublimation cycle
89 of water and carbon dioxide ices on the surface and in the regolith below. The
90 model regolith is composed of equal spherical sand, or dust grains mantled by
91 ice, when it is present. The assumption of perfect sorting of the grains makes
92 the model more appropriate for dunes than for hills of unknown origin. How-
93 ever, for the diffusion of vapor in the regolith most important is size of small
94 grains, filling gaps between larger ones. Hence, the size of grains composing our
95 model hill can be considered as the size of smallest grains in a more realistic
96 hill. In the numerical model are included: the time dependent illumination, in-
97 frared emission from the surface, heat and vapor transport within the regolith
98 as well as the heat exchange due to sublimation or condensation. The flux of
99 absorbed light depends on the local orientation of the surface and on the cur-
100 rent position of the sun. The latter evolves due to orbital motion and rotation
101 of Mars. The model includes warming of the surface due to absorption of: (i)
102 the solar light, direct and scattered in the atmosphere; (ii) the light scattered
103 once within the considered trench, gully or crater; (iii) the IR radiation emit-
104 ted by the atmosphere toward surface. The seasonal and diurnal variations of
105 atmospheric pressure, humidity and atmospheric opacity can be taken either
106 from the results of a general circulation model (GCM), or parameterized.

107 In the current work profiles of the atmospheric pressure, and the atmospheric
108 humidity are taken from the results of GCM LMD/Oxford available at [http://www-](http://www-mars.lmd.jussieu.fr/)
109 [mars.lmd.jussieu.fr/](http://www-mars.lmd.jussieu.fr/)(4 values per sol), for one location at the latitude where
110 the hill-gullies are mostly observed i.e. 50° S. The IR flux emitted from the
111 atmosphere toward the surface is either ignored, or taken from the results of
112 GCM. In the latter case we take diurnal average values averaged over intervals
113 30° L_s. For the atmospheric opacity use of the accurate current profile is not
114 appropriate for our analysis. Opacity of the Martian atmosphere significantly
115 changes from year to year, and the investigated gullies formed in an unknown

116 past. Given this uncertainty we decided to perform two types of simulations.
 117 First one with very low opacity of 0.05 resulting in that the solar flux reaching
 118 the surface is relatively high. Second keeping the opacity at the same low value
 119 but adding IR emission in the atmosphere as calculated for a normal dust at-
 120 mosphere with opacity taken from GCM simulations. This overestimates total
 121 flux of radiation absorbed at the surface and hence gives an upper estimate
 122 of the surface temperature.

123 The equations, except the formula for the instantaneous thickness of the liquid
 124 water film described below, were described in detail in our previous papers
 125 (Kossacki and Markiewicz, 2004; Kossacki et al., 2006). The main equations
 126 are those describing the diffusion of heat in the regolith, and the local energy
 127 input at the surface.

128 2.2 Interfacial melting

129 The actual melting temperature of ice covering regolith grains depends on
 130 the distance to the grain-ice interface. When micron scales or smaller are of
 131 interest, as they are here, effects of short range van der Waals forces need to be
 132 included. Following Moehlamann (2008) pressure resulting from presence of
 133 van der Waals force acting between a mineral grain and the ice layer mantling
 134 is,

$$135 \quad p_{vdW} = \frac{A_H}{6\pi d^3}, \quad (1)$$

136 where A_H is the Hamaker constant and d is the thickness of the liquid film
 137 separating ice layer and the mineral substrate. The excess of pressure resulting
 138 in the interfacial melting can be related to the actual melting temperature via
 139 (Dash et al., 2006),

$$140 \quad \Delta p = H \varrho_l \frac{T_m - T}{T_m}, \quad (2)$$

141 where H is the latent heat of melting, T_m is the standard melting temperature,
 142 and ϱ_l is density of liquid water. Combining the two above equations gives,

$$143 \quad d = \left(\frac{A_H T_m}{6\pi H \varrho_l (T_m - T)} \right)^{1/3}. \quad (3)$$

144 For more details see the two references above and Kereszturi et al. (2009).

145 2.3 Initial and boundary conditions

146 Since we are interested to solve the problem before a gully has formed we will
 147 assume the slope of the considered hill or dune to be a perfect inclined plane.
 148 It is than sufficient to solve heat and the vapor transport equations in one
 149 dimension in the direction perpendicular to the surface. In such case, most
 150 important boundary conditions are those at the surface of a slope: (i) the sur-
 151 face temperature satisfies heat balance through the energy equation (including
 152 heat of sublimation/condensation of a surface ice); (ii) vapor pressure at the
 153 surface (to calculate diffusion of vapor within regolith) is determined by the
 154 atmospheric humidity.

155 The initial volume fraction of ice is: (i) zero at the surface, (ii) linear function
 156 of depth z up to $z = 5$ cm (from 0 at the surface to $v_{i,0}$ at $z = 5$ cm), (iii)
 157 constant with the value $v_{i,0}$, when $z > 5$ cm. For the results presented below
 158 the value of $v_{i,0}$ is 0.30, or 0.01.

159 3 Parameters

160 Key model parameters are summarized in Table 6. The model slope is inclined
 161 by the angle γ toward the pole, or toward the equator. The values of γ are
 162 within the range $5^\circ - 45^\circ$. The regolith is composed of single size spherical
 163 grains whose radii r_g are within the range $50 \mu\text{m} - 0.5$ mm. If it is not stated
 164 otherwise, $r_g = 50 \mu\text{m}$. When the regolith is free of ice, it has the density
 165 $\rho = 1300 \text{ kg m}^{-3}$, the specific heat $c = 820 \text{ J kg}^{-1} \text{ K}^{-1}$, the porosity $\psi = 0.47$.
 166 The thermal conductivity λ of the regolith free of ice is $10 - 50 \text{ mW m}^{-1} \text{ K}^{-1}$.
 167 It is not known, what is the amount of the subsurface ice in locations, where
 168 the hill gullies and dune gullies are observed. It is likely, that dunes are almost
 169 free of ice, but within hills ice may be abundant. In our work we consider two
 170 initial values of the volume fraction of ice: 0.3, and 0.01. Presence of ice in
 171 the regolith enhances most significantly the efficiency of the heat transport.
 172 Thermal conductivity of the solid matrix of grains is determined by the contact
 173 areas of the grains, hence it is a strong function of the volume fraction of ice v_i .
 174 In addition, heat is transported within pore space. In our model the effective
 175 heat conductivity accounts for two processes: (i) heat conduction within the
 176 solid matrix of grains, and (ii) heat transport related to the sublimation and
 177 condensation of vapor in pores. The latter makes the effective conductivity
 178 very sensitive to the temperature. When $\lambda = 10 \text{ mW m}^{-1} \text{ K}^{-1}$, we have for
 179 example:

$$180 \lambda_{eff}(T = 230K) = 0.1 \text{ W m}^{-1} \text{ K}^{-1},$$

$$181 \lambda_{eff}(T = 250K) = 1.5 \text{ W m}^{-1} \text{ K}^{-1},$$

$$182 \lambda_{eff}(T = 270K) = 7.8 \text{ W m}^{-1} \text{ K}^{-1}.$$

183 Fig. 2 shows the temperature dependence of the various components of the
 184 thermal conductivity.

185 The albedo A of a surface free of frost is 0.15 - 0.25, and the emissivity e is
 186 within the range 0.5 - 0.8. For all the results below $A = 0.15$, and $e = 0.8$,
 187 maximizing the film thickness. The Hamaker constant A_H is most likely about
 188 $1.8 \cdot 10^{-19}$ J, but can be as high as 10^{-18} J (Moehlmann, 2008). Here we take
 189 this higher value to maximize the calculated thickness of the liquid layer.
 190 Thickness of a single monolayer of the water molecules is $\delta = 3.5 \cdot 10^{-10}$ m.

191 The simulations are performed with spatial resolution comparable to the di-
 192 urnal thermal skin depth d_{th} . When the regolith is free of ice, the thermal skin
 193 depth is about 1 cm. However, when the regolith contains ice d_{th} becomes an
 194 order of magnitude larger. This change is due to influence of the presence of
 195 ice on the effective heat conductivity. At the temperature 230 K the thermal
 196 skin depths is 8 cm, while close to the melting point it becomes about 40 cm.
 197 The size of the grid itself is adjusted to have the vertical temperature gradient
 198 at the bottom boundary negligibly small. We performed tests and found, that
 199 10 meters is sufficient. Resolution of our simulations is 1.25 - 10 cm and the
 200 time step is 2 - 30 seconds.

201 4 Results

202 In this section we present the simulated diurnal and seasonal cycles of the
 203 water film thickness in the regolith. The former is shown for $L_s = 271^\circ$, while
 204 the latter for $L_s = 180^\circ - 280^\circ$. Figures 3 - 5 show results of these simulations
 205 for slopes facing North and South. The values of other parameters are: the
 206 regolith dry thermal conductivity $\lambda = 50$ mW/m/K, the volume fraction of
 207 ice $v_{i0} = 0.3$, ice free surface albedo $A = 0.15$, and the emissivity $\epsilon = 0.8$.
 208 These values are chosen to maximize the film thickness meaning that all the
 209 values except albedo are at the high end of their possible range and albedo
 210 is low. Figure 3 shows diurnal profiles of the temperature of the regolith,
 211 while Figures 4 and 5 show diurnal profiles of the thickness of the interfacial
 212 water film. The curves are drawn for different depths beneath a flat slope
 213 inclined by either 25° or 35° (temperature profiles are shown only for 25°).
 214 The atmospheric humidity is taken from the GCM results for the present
 215 climate. The surface of the equator facing slope warms up in the afternoon up
 216 to 320 K, about 50 K above the melting temperature of pure water ice. At the
 217 depth of 2.5 cm temperature reaches nearly 270 K, which is reflected in growth
 218 of the interfacial water film to almost 10 monolayers (Figure 4, lower panel).
 219 This thickness persists for a time of several tens of minutes. At this depth
 220 the film of thickness of about 5 monolayers can be expected to be present for
 221 about 5 hours. The drop of the film thickness at about 4 pm is due to complete

222 sublimation of ice. Deeper below the surface the temperature is significantly
223 lower throughout the whole day and thickness of the liquid layer is at the most
224 3 monolayers. When a slope is inclined toward the pole, all temperatures are
225 lower and the maximum film thickness is only about 3 monolayers even at the
226 depth of 2.5 cm. In Figures 4 - 5 we show diurnal cycle of the film thickness
227 for slopes inclined by 35° (upper panels). The values are somewhat lower than
228 for the case of 25° but the dependence on this parameter is not very strong.

229 In Figures 6, and 7 we show diurnal cycle of the interfacial water film thickness,
230 when the model also includes absorption of the IR flux from the atmosphere.
231 We see that this additional heating causes film thickness at depth of 2.5 cm
232 on the equator facing slope to grow rapidly followed by complete sublimation
233 of ice already at about 10:30 AM. Judging from the curve for 5 cm depth we
234 can expect that the result at about 3 cm should be similar to that at 2.5 cm
235 when atmospheric heating is not included.

236 In Figure 8 we show the seasonal evolution of the diurnal maximum of the
237 liquid film thickness for both slope orientations. The profiles are shown for
238 two values of slope inclination and with and without additional atmospheric
239 heating. They are for depth of 5 cm for the equator facing slope and depth
240 of 2.5 cm for the pole facing one. We see that the largest thickness of nearly
241 10 monolayers occurs on the equator facing slope and persists for about 40
242 martian days.

243 To investigate potential importance of liquid water films for the formation
244 of dune gullies we have also calculated models with very low initial volume
245 fraction of subsurface water ice of 0.01. We considered two locations, namely,
246 (50°S , 50°E) and (50°S , 135°E). The former is in the Hellas basin, while the
247 latter is on the southern highland. These locations differ in atmospheric pres-
248 sure and humidity. For both locations during summer water ice is permanently
249 present only at depths larger than 10 cm. Closer to the surface ice condenses
250 at night (due to diffusion of the vapor from above or below, or freezing of
251 water adsorbed on the mineral grains), and sublimates away during the day.
252 The remaining model parameters are the same as in the case of Fig. 4. The
253 diurnal maximum of the water film thickness obtained is always less than 4
254 monolayers and roughly the same for both locations. This indicates, that the
255 atmospheric pressure and humidity have minor effect. Comparison with the
256 profiles presented in Fig. 4 shows, that the water film thickness is at the depth
257 of 2.5 cm is about 2 times smaller than predicted for the regolith rich in ice.
258 The seasonal cycles are not significantly different for the two cases, only that
259 ice poor regolith has never more than 4 monolayers film thickness. We have
260 also looked at the dependence on grain and did not find this parameter to be
261 in any way critical.

262 5 Conclusions

263 We attempted to answer the question, whether an interfacial water film of
264 significant thickness may form in locations where the hill-gullies are observed.
265 We investigated interfacial melting in the regolith beneath the sloped surfaces
266 at a depth of few centimeters. We considered different initial volume fraction
267 of the subsurface ice: high, possible for gullied hills, and low, likely for dunes.

268 When the regolith is rich in ice, our simulations suggest that under extreme
269 conditions one may expect formation of a liquid film of water about 10 mono-
270 layers thick. Calculating stability of a slope in a presence of moisture is beyond
271 the scope of the current work. However, quick estimate suggests, that 10 mono-
272 layers of liquid water could be sufficient to make the surface layer unstable.
273 If we take thickness of the monolayer to be $3.5 \cdot 10^{-10}$ m, the whole liquid film
274 is only $3.5 \cdot 10^{-9}$ m thick. We can compare this to the expected roughness of
275 the grains within the regolith. The smallest grains are about 1 micron in size.
276 Assuming the surface irregularities are 1% (10^{-8} m), we would require about
277 30 monolayers to fill them, which could allow films of neighbouring grains to
278 connect. Although this is more than we observe in the model, we should note
279 that: (i) it is of the same magnitude and given model limitations should be
280 considered similar; and (ii) full separation of the adjacent grains may be not
281 necessary for the material on a steep slope to become unstable. It should also
282 be noted that gullies (of any type) found in mid-latitudes are mostly equa-
283 torial facing (Balme et al., 2006) orientation for which we also find thicker
284 interfacial water films.

285 When the regolith contains low amount of ice, formation of a thick water film
286 solely due to local interfacial melting is very unlikely. At the equatorward
287 oriented slope interfacial water appears few centimeters beneath the surface
288 only in the coldest season, in sommer the regolith remains dry. At the poleward
289 inclined slope interfacial water may appear the whole year but the liquid film
290 is thin. Hence, only periodical sinking of water to a colder layer, freezing and
291 melting seems to be able to produce significant amount of liquid water, as
292 suggested by Kereszturi et al. (2010).

293 6 Acknowledgments

294 This work was partially supported by the Polish Ministry of Education and
295 Science (grant 0576/H03/2007/32).

296 References

- 297 Balme M., Mangold N., Baratoux D., Costard F., Gosselin M., Masson P.,
298 Pnet P., and Neukum G., 2006. Orientation and distribution of recent gul-
299 lies in the southern hemisphere of Mars: Observation from High Resolu-
300 tion Stereo Camera/Mars Express (HRSC/MEX) and Mars Orbiter Cam-
301 era/Mars Global Surveyor (MOC/MGS) data. *J. Geophys. Res.*, 111 doi:
302 1029/2005JE002607
- 303 Christensen, P., 2003. Formation of recent martian gullies through melting of
304 extensive water-rich snow deposits. *Nature*, 422, 45-48
- 305 Costard, F., Forget F., Mangold N., and Peulvast J. P., 2002. Formation of
306 Recent Martian Debris Flows by Melting of Near-Surface Ground Ice at
307 High Obliquity. *Science*, 295, 110–113
- 308 Dash J.G., Rempel A.W., and Wettlaufer J.S., 2006. The physics of premelted
309 ice and its geophysical consequences. *Reviews of Modern Physics*, 78, 695-
310 741
- 311 Fenton, L., 2006. Dune migration and slip face advancement in the
312 Rabe crater dune field, Mars. *Geophys. Res. Lett.* 33. L20201.
313 doi:10.1029/2006GL027133.
- 314 Hecht, M. 2002. Metastability of liquid water on Mars. *Icarus*, 156, 373–386.
- 315 Heldmann J. L., Carlsson E., Johansson H., Mellon M. T., and Toon, O. B.,
316 2007. Observations of martian gullies and constraints on potential formation
317 mechanisms. *Icarus*, 188, 324-344
- 318 Ingersoll, A.P., 1970. Mars: Occurrence of Liquid Water. *Science*, 168, 972–973
- 319 Ivanov, A. B., and D. O. Muhleman, 2000. The Role of Sublimation for the
320 Formation of the Northern Ice Cap: Results from the Mars Orbiter Laser
321 Altimeter. *Icarus*, 144, 436–448.
- 322 Jaumann, R., Neukum, G., Behnke, T., Duxburry, T.C., Eichertopf, K., van
323 Gasselt, S., Giese, B., Gwinner, K., Hauber, E., Hoffmann, H., Hoffmeister,
324 A., Khler, U., Matz, K.-D., McCord, T.B., Mertens, V., Oberst, J., Pis-
325 chel, R., Rei, D., Ress, E., Roatsch, T., Saiger, P., Scholten, F., Schwarz,
326 G., Stephan, K., Whlisch, M., and the HRSC Co-Investigator Team, 2007.
327 The High Resolution Stereo Camera (HRSC) Experiment on Mars Express:
328 Instrument Aspects and Experiment Conduct from Interplanetary Cruise
329 through Nominal Mission. *Planet. Space Sci.*, 55, 928-952.
- 330 Kereszturi, A., Mhlmann, D., Berczi, Sz., Ganti, T., Kuti, A., Sik, A., Horvath,
331 A., 2009. Recent rheologic processes on dark polar dunes of Mars: Driven
332 by interfacial water? *Icarus* 201, 492503.
- 333 Kereszturi, A., Mhlmann, D., Berczi, Sz., Ganti, T., Horvath, A., Kuti, A.,
334 Sik, A., Szathmary, E., 2010. Indications of brine related local seepage phe-
335 nomena on the northern hemisphere of Mars. *Icarus* 207, 149-164.
- 336 Mhlmann, D., Kereszturi, A., 2010. Viscous liquid film flow on dune slopes of
337 Mars. *Icarus*, doi:10.1016/j.icarus.2010.01.002
- 338 Kossacki K.J., and Markiewicz W.J., 2004. Seasonal melting of surface water

- 339 ice condensing in martian gullies. *Icarus*, 171, 272-283
- 340 Kossacki K. J., Markiewicz W. J., Smith M. D., Page D., Murray J, 2006.
- 341 Possible remnants of a frozen mud lake in southern Elysium, Mars. *Icarus*,
- 342 181, 363-374
- 343 Kossacki K. J., and Markiewicz, W.J., 2009. Small-scale trench in the north
- 344 polar region of Mars: Evolution of surface frost and ground ice concentra-
- 345 tion. *Icarus*, 199, 75-85
- 346 Malin, M. C. and K. S. Edgett, 2000. Evidence of recent groundwater seepage
- 347 and surface runoff on Mars. *Science*, 288, 2330.
- 348 Mangold, N., Costard, F., Forget, F., 2003. Debris flows over sand dunes on
- 349 Mars: Evidence for liquid water. *J. Geophys. Res.*, 108, E4, pp. 8-1, DOI
- 350 10.1029/2002JE001958
- 351 Mellon, M. T., and R. J. Philips, 2001. Recent gullies on Mars and the source
- 352 of liquid water. *J. Geophys. Res.*, 106, 23,165–23,180
- 353 Miyamoto, H., Dohm, J.M., Baker, V.R., Beyer, R.A., and Bourke, M., 2004.
- 354 Dynamics of unusual debris flows on Martian sand dunes. *Geophys. Res.*
- 355 *Lett.*31, L13701, doi:10.1029/2004GL020313.
- 356 Moehlmann D., 2008. The influence of van der Waals forces on the state
- 357 of water in the shallow subsurface of Mars. *Icarus*, in press, DOI:
- 358 10.1016/j.icarus.2007.11.026
- 359 Neukum, G., Jaumann, R., and the HRSC Co-Investigator and Experiment
- 360 Team, 2004. HRSC: The High Resolution Stereo Camera of Mars Express,
- 361 in *Mars Express: The scientific payload*, edited by A. Wilson, pp. 17-35,
- 362 ESA, Noordwijk, The Netherlands.
- 363 Paterson, W. S. B., in *The Physics of Glaciers*, Elsevier, New York, 1994
- 364 Reiss, D., Jaumann, R., Kereszturi, A., Sik, A., and Neukum G., 2007. Gullies
- 365 and avalanche scars on Martian dark dunes. *Lunar Planet. Sci.*, XXXVIII,
- 366 Abstract 1993.
- 367 Reiss, D., Erkeling, G., Bauch, K. E., Hiesinger, H., 2010. Evidence for present
- 368 day gully activity on the Russell crater dune field, Mars. *Geophys. Res.*
- 369 *Lett.*37, L06203, doi:10.1029/2009GL042192.
- 370 Toon, O.B., Pollack, J.B., Ward, W., Burns, J. A., and Bilski, K., 1980. The
- 371 astronomical theory of climatic change on Mars. *Icarus*, 44, 552-607
- 372 Williams, K. E., Toon, O. B., Heldmann, J. L., McKay, C., and Mellon, M.
- 373 T., 2008. Stability of mid-latitude snowpacks on Mars *Icarus*, 196, 565-577.

374 Table 1 (File: I11326_table.tex)

375

ACCEPTED MANUSCRIPT

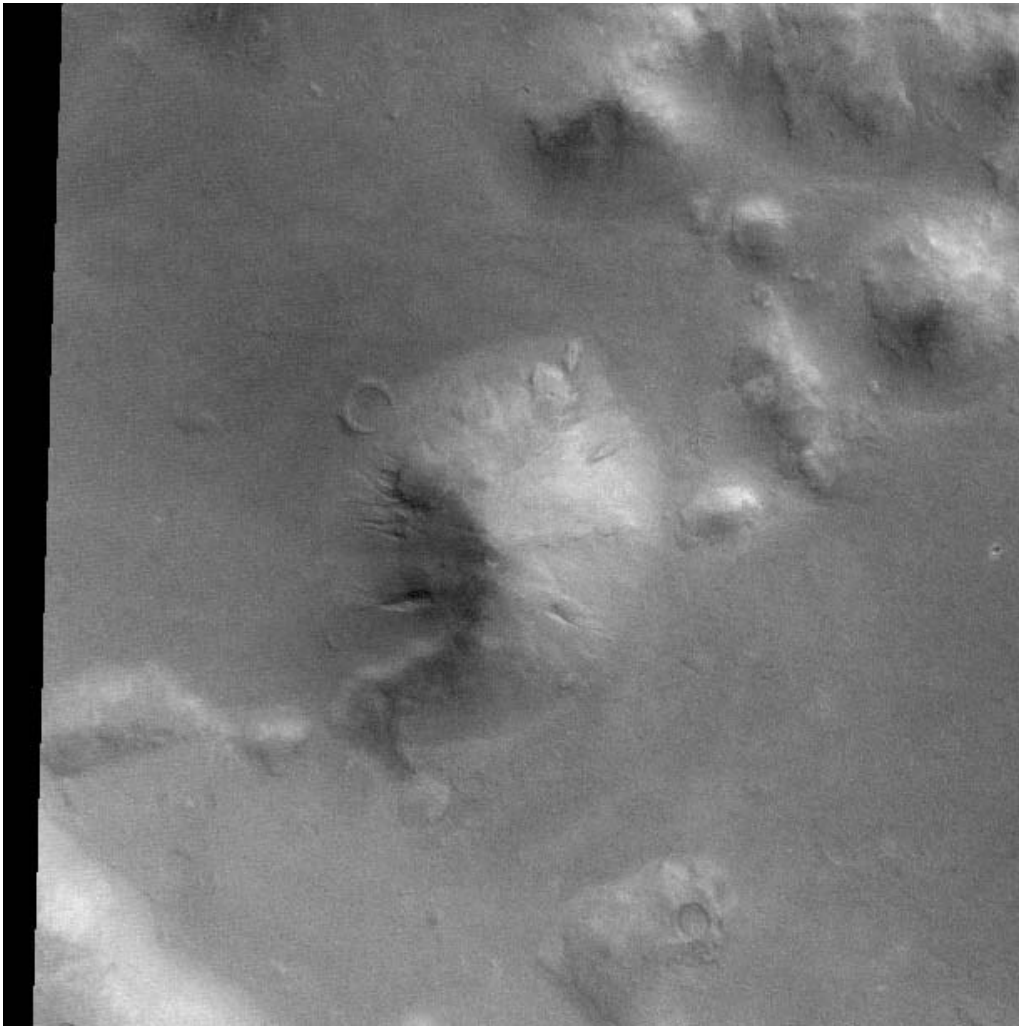


Fig. 1. Part of HRSC image h0155-000 showing gullies on slopes of a hill located approximately at 47.25°S , and 330.1°E . The hill is about 1 km across, and about 1 km high. North is up. The image comes from HRSCview. Freie Universitaet Berlin and DLR Berlin, <http://hrscview.fu-berlin.de/>. See also Neukum et al. (2004); Jaumann et al. (2007).

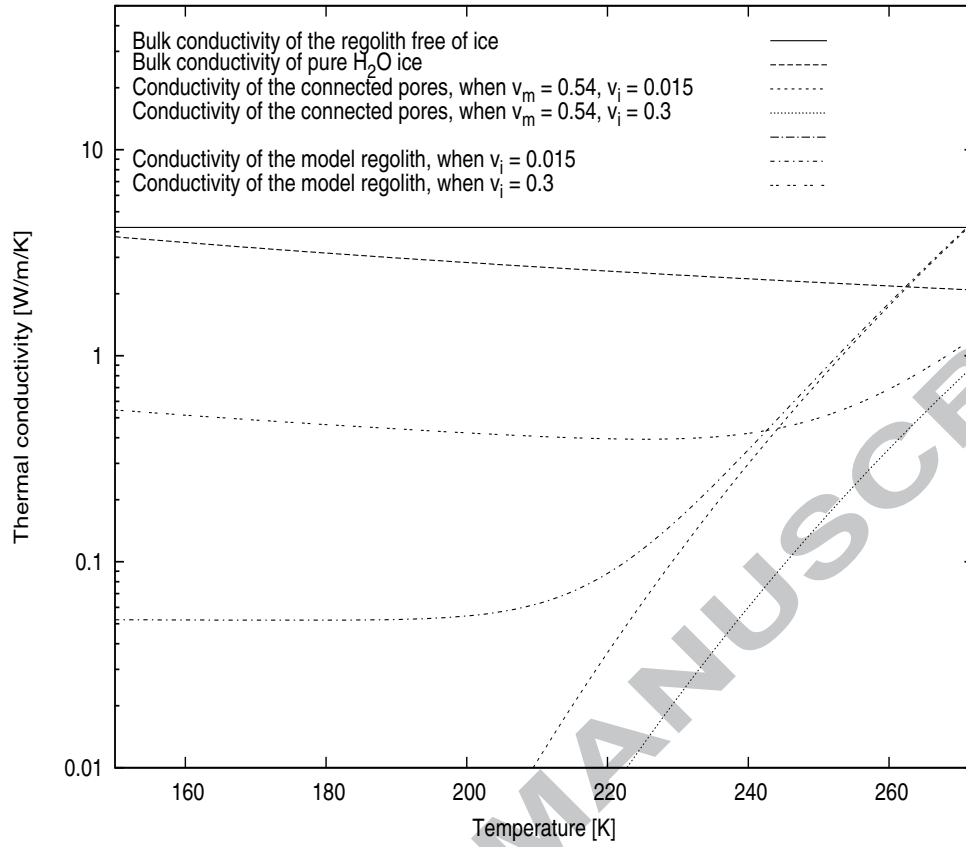


Fig. 2. Thermal conductivity of a regolith composed of grains covered by water ice.

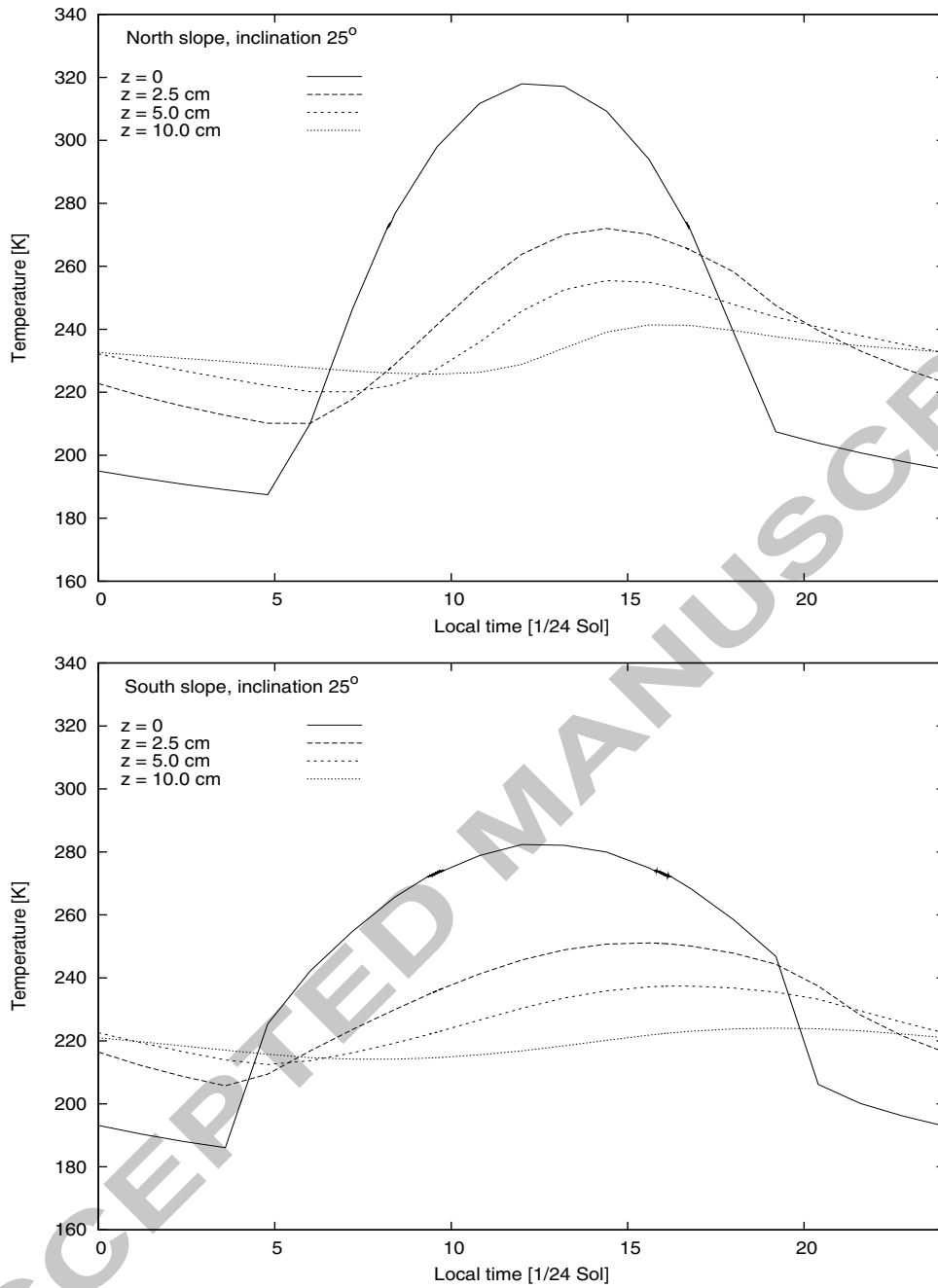


Fig. 3. Diurnal cycle of the temperature at different depth, when the slope is inclined toward North (upper panel), and toward South (lower panel). The profiles are drawn for $L_s = 271^\circ$.

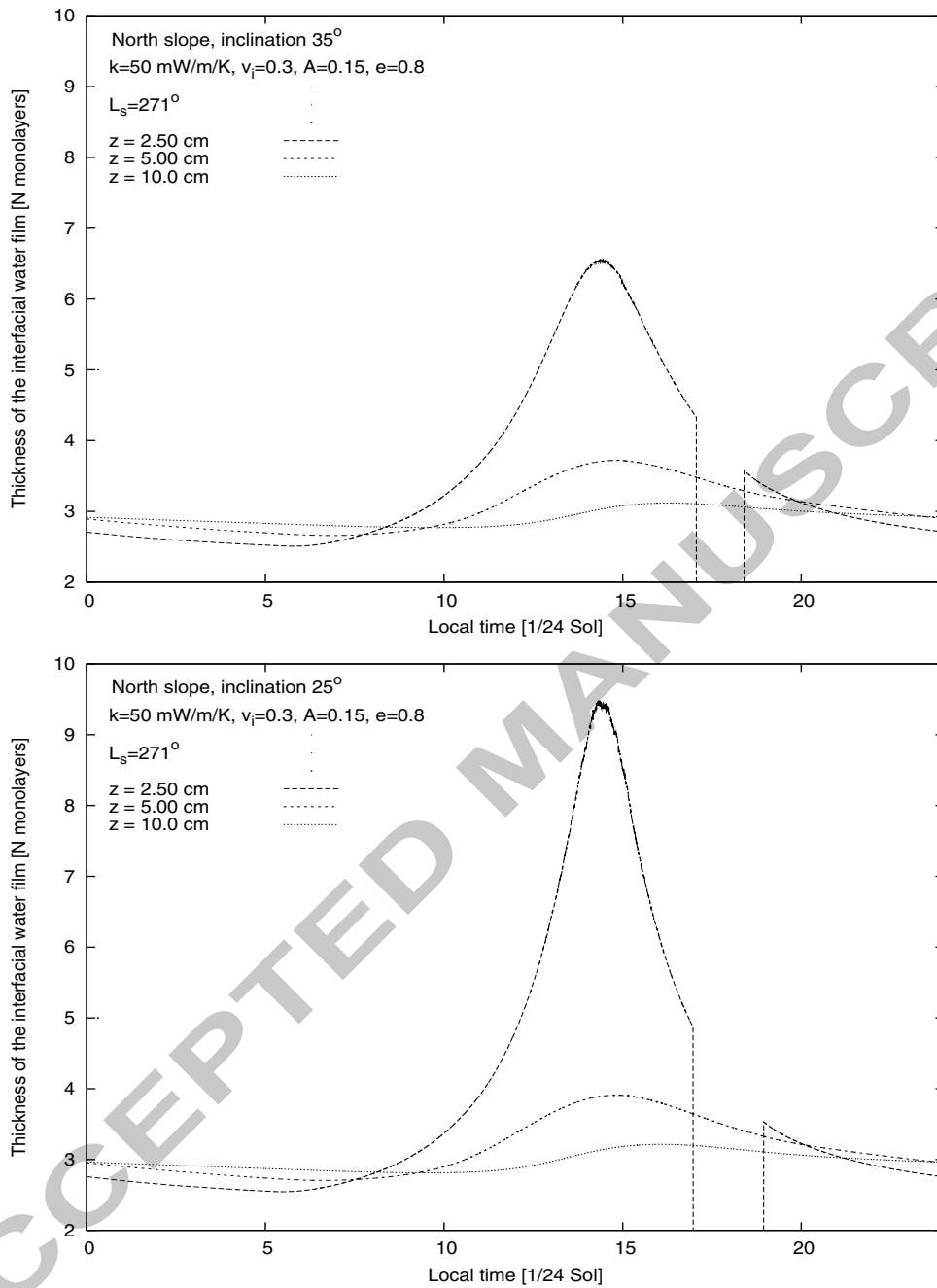


Fig. 4. Diurnal cycle of the thickness of the interfacial water film on regolith grains. The slope is inclined toward North by 35° (upper panel), and 25° (lower panel). The profiles are drawn for $L_s = 271^\circ$.

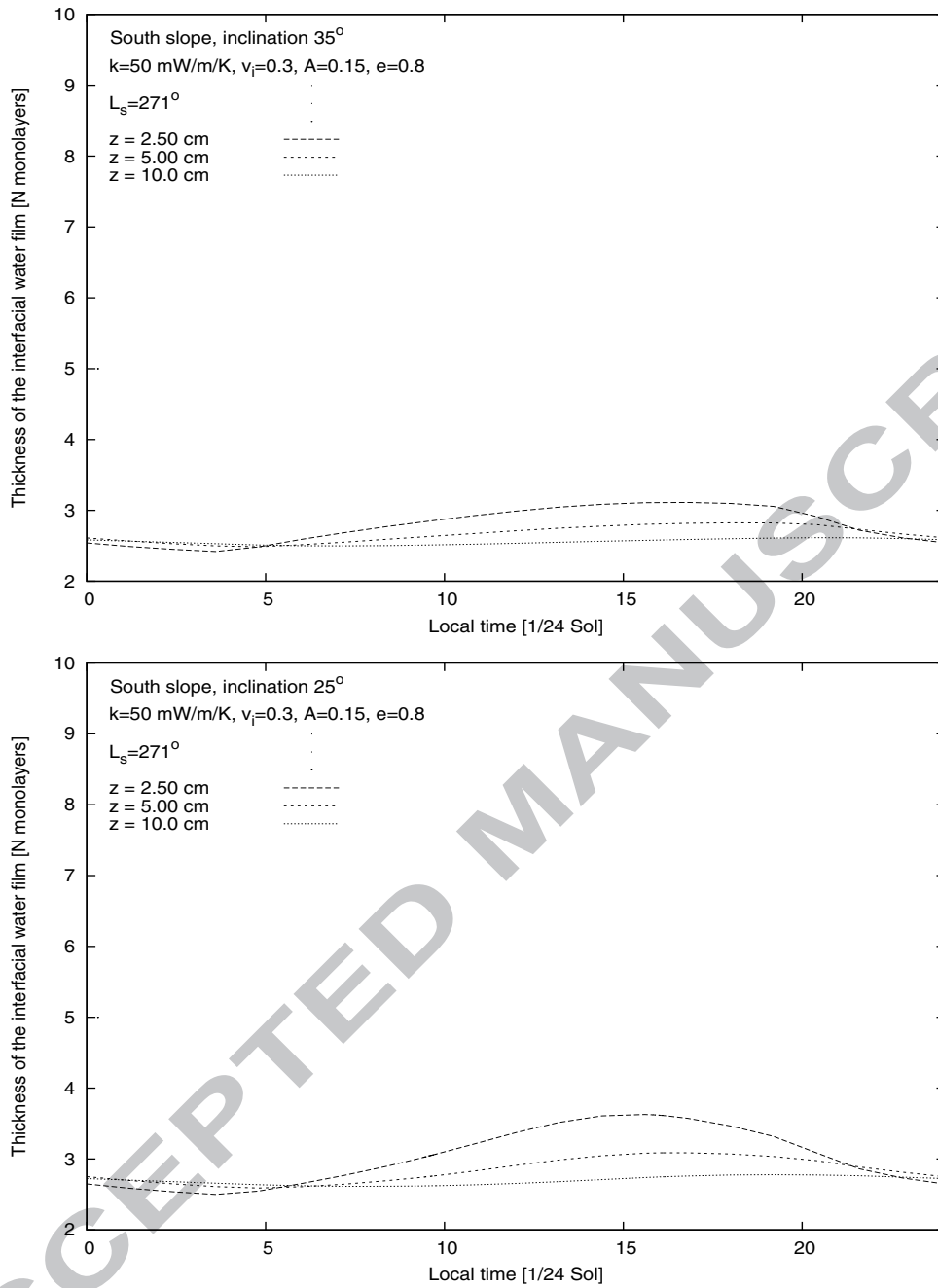


Fig. 5. The same as in Fig. 4, but for a south facing slope.

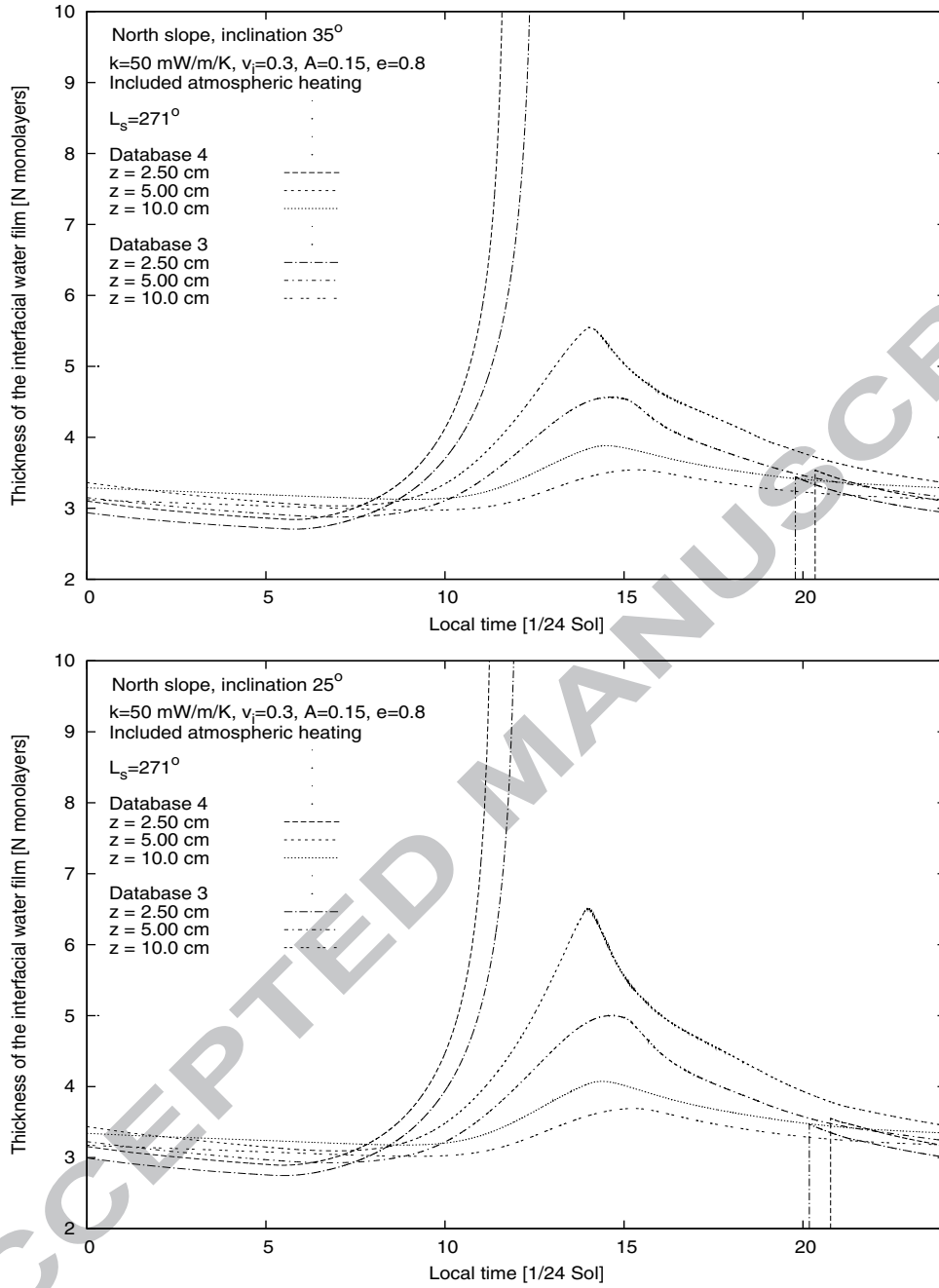


Fig. 6. Diurnal cycle of the thickness of the interfacial water film on regolith grains, as in Fig. 4, but including the IR flux from the atmosphere toward surface. The latter is taken from the results of the GCM LMD/Oxford, databases: 3 and 4. The profiles are drawn for $L_s = 271^\circ$.

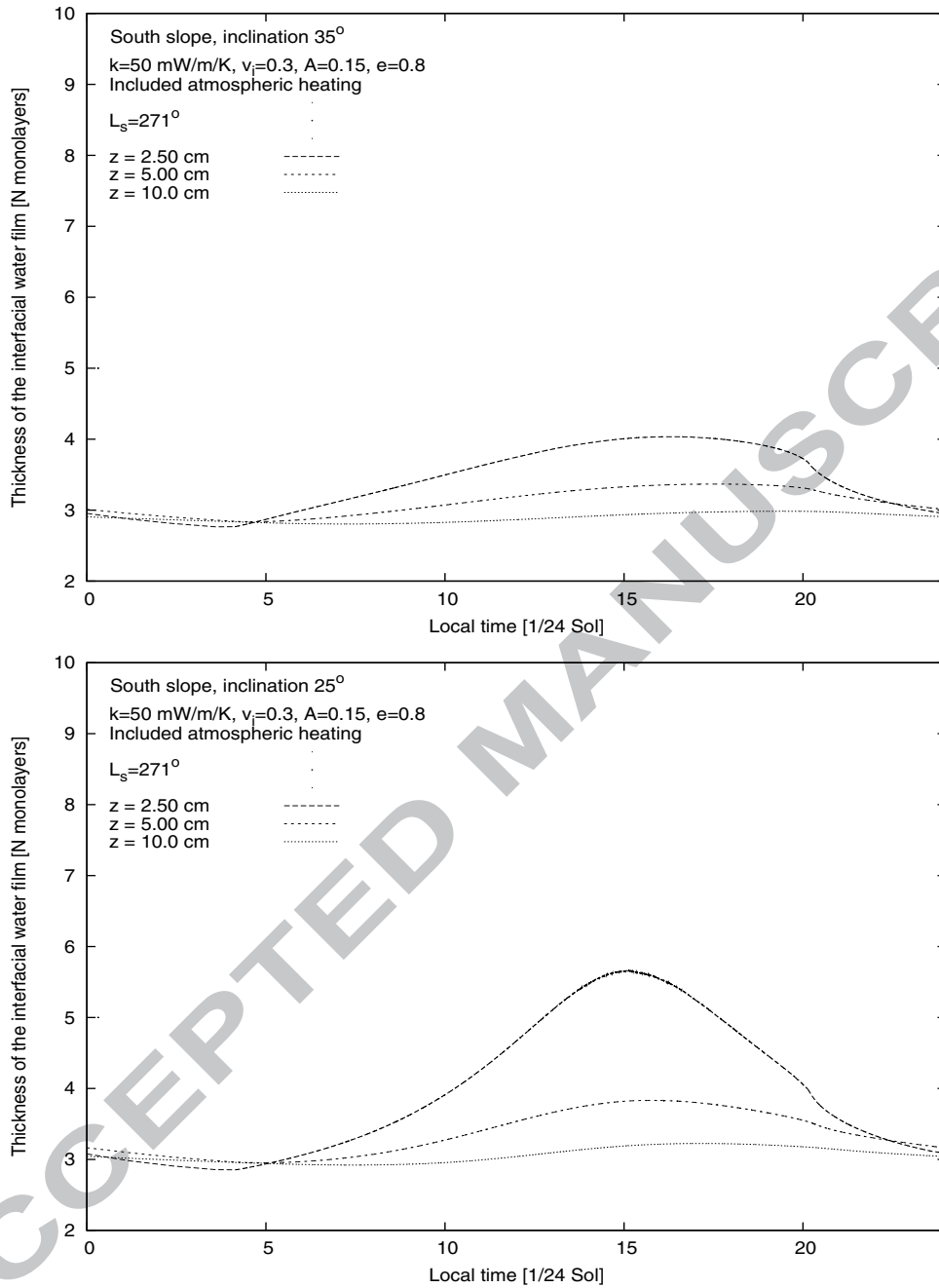


Fig. 7. The same as in Fig. 5, but including the IR flux from the atmosphere toward surface.

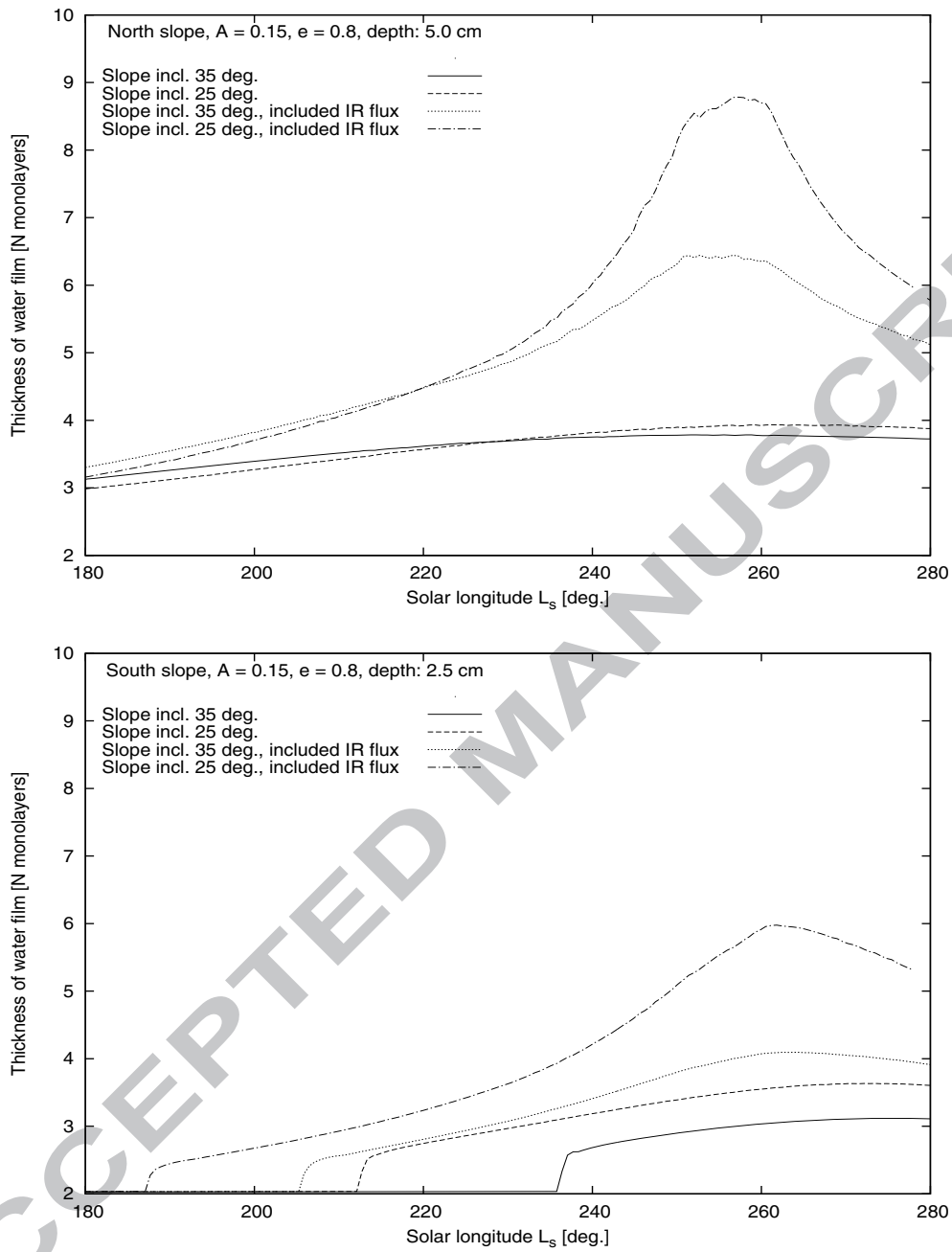


Fig. 8. Seasonal dependence of the diurnal maximum of the interfacial water film thickness, when: (i) equator facing slope, at depth $z = 5$ cm (upper panel); (ii) poleward facing slope, at depth $z = 2.5$ cm (lower panel).

Table 1
Model parameters

Parameter	Symbol	Units	Value
Albedo of the regolith free of ice	A		0.15
Albedo of the regolith covered by thick ice	A_i		0.35
Emissivity of the regolith free of ice	ϵ		0.8
Emissivity of the regolith covered by thick ice	ϵ_i		0.65
Grain/pore radius free of ice	$r_g = r_p$	[mm]	0.05
Density of the regolith	ρ	[kg m ⁻³]	1300
Thermal conductivity of the regolith free of ice	λ	[W m ⁻¹ K ⁻¹]	0.05
Initial volume fraction of ice	v_{i0}		0.3, 0.01
Porosity of the regolith when free of ice	$\psi = 1 - v_m$		0.46
Specific heat of the regolith free of ice	c_m	[J kg ⁻¹ K ⁻¹]	820
Hamaker constant	A_H	[J]	$10^{-19} - 10^{-18}$
Thickness of a single monolayer of the water molecules	δ	[m]	$3.5 \cdot 10^{-10}$
Inclination of a hill slope	γ	[°]	15 - 35